www.sciencemag.org/cgi/content/full/science.1254917/DC1

Supplementary Materials for

Poly-dipeptides encoded by the C9ORF72 repeats bind nucleoli, impede RNA biogenesis, and kill cells

Ilmin Kwon, Siheng Xiang, Masato Kato, Leeju Wu, Pano Theodoropoulos, Tao Wang, Jiwoong Kim, Jonghyun Yun, Yang Xie, Steven L. McKnight*

*Corresponding author. E-mail: steven.mcknight@utsouthwestern.edu

Published 31 July 2014 on *Science* Express
DOI: 10.1126/science.1254917

This PDF file includes

Other Supplementary Material for this manuscript includes the following:
(available at www.sciencemag.org/cgi/content/full/science.1254917/DC1)

Table S1. RNA-seq data of human astrocytes exposed to PR_{20} synthetic peptide. As an Excel spreadsheet.

Materials and Methods

Hydrogel-binding assays

Hydrogel droplets of mCherry:hnRNPA2 were prepared as described previously (*10, 11*). For hydrogel binding assay, purified GFP-fused proteins were diluted to 1 μM and applied to the chamber slides containing mCherry:hnRNPA2 hydrogel droplets. After overnight incubation at 4˚C, mCherry:hnRNPA2 hydrogel droplets and trapped GFP fusion proteins were detected by Leica TCS SP5 confocal microscopy. For CLK kinase assay on GFP-fusion proteins pre-bound to mCherry hydrogel droplets, the solution of GFP-fused protein was removed from the hydrogel droplets after overnight incubation at 4˚C and then the reaction mixtures containing CLK1 or CLK2 (Millipore) in kinase reaction buffer (50 mM Mops-NaOH pH7.0, 1 mM EDTA, 0.001% NP-40, 2.5% glycerol, 0.05% BME) in the presence or absence of ATP were immediately added to the hydrogel droplets. After overnight incubation at room temperature, hydrogel droplets were analyzed by Leica TCS SP5 confocal microscopy.

Protein purification

For construction of bacterial expression plasmids of GFP:SRSF2 or GFP:$SRSF2_{G1/G2}$, DNA fragments encoding SR domain (residue 101-221) of SRSF2 or $SRSF2_{G1/G2}$, respectively were cloned into pHis-GFP parallel vector (*29*). To generate bacterial expression plasmids of GFP-fused SR_{20}, GR_{20} or PR_{20}, DNA fragments encoding 20 repeats of SR, GR or PR were synthesized from GeneWiz (NJ) and were cloned into pHis-GFP-parallel vector. All recombinant proteins were expressed in *E. coli* strain BL21 (DE3) and purified as previously described (*11*).

Peptide synthesis

Peptides contain 20 repeats of GR or PR (GR_{20} or PR_{20}, respectively) with an HA epitope tag at the C-termini were synthesized from the Protein Chemistry Core at UT Southwestern Medical Center. Peptides were synthesized on an Applied Biosystems 433 automated peptide synthesizer (Foster City, CA) using optimized Fmoc chemistry as described elsewhere (*30*). Crude peptides were purified on a Waters 600 HPLC system (Milford, MA) using a Vydac C18 semi-preparative column (250mmx10mm) at 3ml/min and 0-100% B in 120 min, where A is water/0.045% TFA and B is acetonitrile/0.036% TFA. The purified peptides were characterized using ESI-MS.

Cell viability

U2OS cells were seeded in 96 well plates at a density of $5x10^3$ cells/well and treated with indicated amount of GR_{20} or PR_{20} peptides. Cells were incubated for indicated time periods at 37˚C with cell viability determined by use of the CellTiter-Glo Luminescent assay (Promega) according to manufacturer's protocol. Briefly, 50 µl of CellTiter-Glo reagent was added to the wells containing 100 µl of growth medium. After vigorous shaking at room temperature for 10 minutes, luminescence was measured to determine cell viability. Cell viability determination was performed in triplicate.

RNA sequencing and data analysis

High-throughput sequencing resulted in 118.8 million paired-reads for the control sample and 98.6 million reads for the PR20 treated sample. NGS QC Toolkit (v2.3.1) was used to check the sequencing quality, and 110.0 million reads (92.7%) for the control sample and 90.8 million reads (92.1%) for the PR20 sample were selected to be used in the following steps. The sequencing data were aligned by TopHat (v2.0.8) (*31*) to hg19 reference genome sequence along with the gene annotation data downloaded from Illumina's iGenomes. For the control sample, 90.7 million reads (82.4%) were mapped concordantly and for the PR20 sample, 74.4 million reads (82.0%) were mapped concordantly. Cufflinks (*32, 33*) was used to quantify the expression levels (FPKM) of both gene and isoform units with frag-bias-correct and multi-read-correct options. We adopted the mode of advanced reference annotation based transcript (RABT) assembly for Cufflinks. To compare RNA abundance between the PR20 sample and the control sample, a normalization method was carried out to avoid bias in estimating the normalization factor, and a negative binomial model was applied to identify significantly differential expressed genes. The expression levels of each isoform for the same gene were compared between conditions to identify alternative splicing evens. The Kolmogorov–Smirnov test was used to compare the distribution difference between the ribosomal protein family and the background distribution with all genes (*34*).

RT-PCR for validation of mis-splicing

Human astrocytes were seeded at density of 10^5 cells/well in 6 well plates. After 24 hours incubation at 37˚C, 10 or 15 µM of the PR_{20} peptide was applied to the cells. After 36 hours of incubation, total RNA was isolated using the RNA Stat-60 reagent (Amsbio) according to the manufacturer's instruction. After DNA digestion using Turbo DNase (Lifetechnologies), 1 µg of RNA was reverse transcribed using Superscript III reverse transcriptase (Lifetechnologies) as per manufacturer's instruction. PCR amplification was performed using PrimeSTAR DNA polymerase (1.25 units/50 µl reaction, Takara). Primers used for PCR analysis of the EAAT2 mRNA were as follow (*23*): EAAT2-A (5'-

GGCAACTGGGGATGTACA-3'); EAAT2-B (5'-CCAGAAGGCTCAAGAAGT-3'); EAAT2-C (5'-ACGCTGGGGAGTTTATTCAAGAAT-3'). For PCR of EAAT2, three primers (EAAT2-A, B, and C) were added in 1:1:1 ratio. For validation of aberrant splicing in RAN, PTX3, NACA, or GADD45A, reverse transcript products from control or PR_{20}-treated human astrocytes was used as template. Primer sequences for each mRNA were as follows: RAN-A (5'-CCATCTTTCCAGCCTCAGTC-3'); RAN-B (5'-GGCTGTGTCCCATACATTGA-3'); PTX3-A (5'-AGCCTCTCACTCTCACTCTC-3'); PTX3-B (5'-CCACCCACCACAAACACTAT-3'); NACA-A (5'-AAGTCGGCAAACGTAGTCCAGG-3'); NACA -B (5'-CTGCTACAGAGCAGGAGTTG-3'); NACA-C (5'-GGCTCTTGTAGACATCTGGTTT-3'); GADD45A-A (5'-TTGTCCTCCAGTGGCTGGTA-3'); GADD45A-B (5'-CGCAGGATGTTGATGTCGTTCT-3').

qPCR for ribosomal RNA processing

Processing of ribosomal RNA in PR_{20} peptide-treated cells was analyzed by qPCR. Human astrocytes were exposed to 10 μM or 30 μM of PR_{20} peptide for 12 hours. A total of 1 μg of DNase-treated RNA was reverse transcribed using random hexamer and Superscript III reverse transcriptase. For qPCR, 1 % of the RT product was used as template. Cyclophilin mRNA level was used as an internal control and the data were plotted as normalized fold-change against control. Primers used to detect the rRNA precursor were as follow: 45S-f (5'-GAACGGTGGTGTGTCGTT-3'); 45S-r (5'-GCGTCTCGTCTCGTCTCACT-3'); 18S-5'-jucntion-f (5'-GCCGCGCTCTACCTTACCTACCT-3'); 18S-5'-jucntion-r (5'-CAGACATGCATGGCTTAATCTTTG-3'); 18S-3'-jucntion-f (5'-AGTCGTAACAAGGTTTCCGTAGGT-3'); 18S-3'-jucntion-r (5'-CCTCCGGGCTCCGTTAAT-3'); 5.8S-5'-jucntion-f (5'-TACGACTCTTAGCGGTGGATCA-3'); 5.8S-5'-jucntion-r (5'-TCACATTAATTCTCGCAGCTAGCT-3'); 5.8S-3'-jucntion-f (5'-GAATTGCAGGACACATTGATCATC-3'); 5.8S-3'-jucntion-r (5'-GGCAAGCGACGCTCAGA-3'); 28S-5'-jucntion-f (5'-CCGAGACGCGACCTCAGAT-3'); 28S-5'-jucntion-r (5'-TCCGCTGACTAATATGCTTAAATTCA-3'). Primers used to detect mature rRNAs were as follow: 18S-f (5'-GATGGTAGTCGCCGTGCC-3'); 18S-r (5'-GCCTGCTGCCTTCCTTGG-3'); 5.8S-f (5'-ACTCGGCTCGTGCGTC-3'); 5.8S-r (5'-GCGACGCTCAGACAGG-3'); 28S-f (5'-GTGACGCGCATGAATGGA-3'); 28S-r (5'-TGTGGTTTCGCTGGATAGTAGGT-3'). Primers used for monitoring the cyclophilin control mRNA were "cyclophilin-f" (5'-TGCCATCGCCAAGGAGTAG-3') and "cyclophilin-r" (5'-TGCACAGACGGTCACTCAAA-3').

Southern blot

For Southern blot analysis of EAAT2 transcripts, 2 μl from a 50 μl of PCR reaction product was resolved on a 1.5% agarose gel. The gel was denatured in denaturing buffer (0.5 M NaOH and 1.5 M NaCl) for 30

min at room temperature. After washing with distilled water, gel was transferred to neutralizing buffer (0.5 M Tris-HCl pH 7.0 and 1.5 M NaCl). After 30 min of neutralization at room temperature, the gel was soaked into 20X SSC transfer buffer (3 M NaCl, 0.3 M Na citrate) for 30 min. PCR bands were transferred onto the Nytran membrane using TurboBlotter (rapid downward transfer system, GE Healthcare) system as manufacturer's protocol. After transfer, the Nytran membrane was baked using UV cross linker. After 1 hour of pre-hybridization in Rapid-hyb buffer (GE Healthcare) at 42˚C in a glass hybridization bottle, a total of $6X10^6$ cpm of ^{32}P end-labeled oligonucleotide probes for either Exon 9-skipping or intron-retention transcripts of the EAAT2 mRNA were applied to the membrane and incubated for 1 hour at 42˚C. After stringent washing, membranes were dried and the bound probes were visualized by autoradiography. Oligonucleotides used to make end-labeled probes were as follow: EAAT2-Exon8/10 junction (5'-TGACTGTAAGGGACAGGATG-3'); EAAT2-Exon7/intron junction (5'-CCGCTTCCAGGTAGAGAACAA-3').

Supplementary Figures

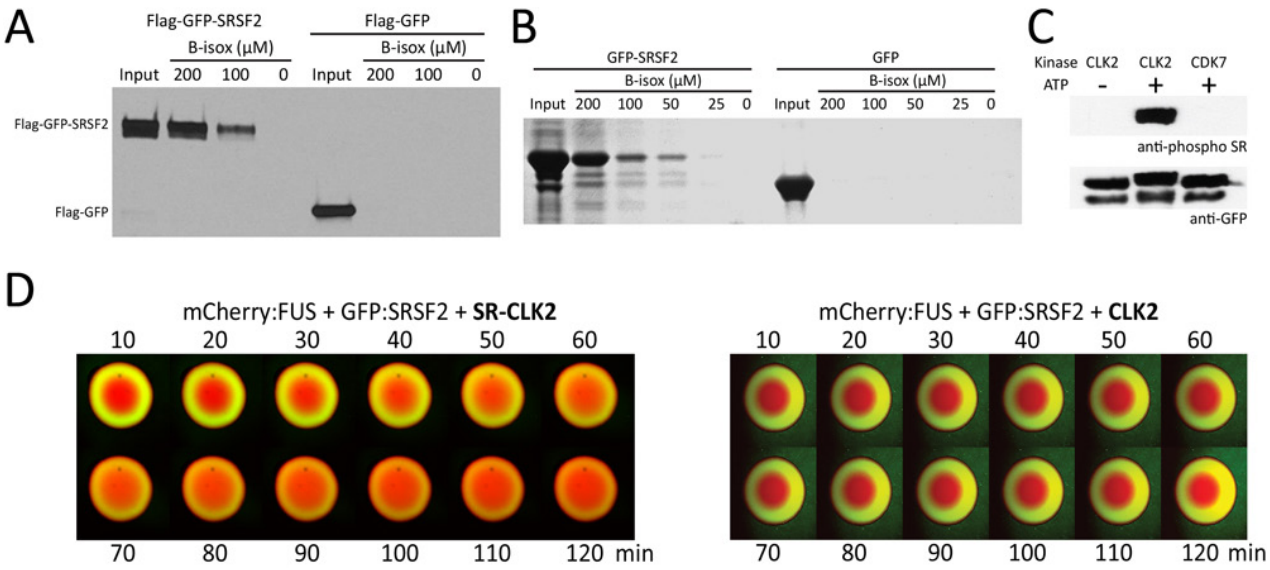

Fig. S1. Biotinylated isoxazole-mediated precipitation of SR domain of SRSF2. (A and B) Flag-tagged GFP and GFP fused to the SR repeats of SRSF2 (amino acids 106 to 144) were exposed to indicated amounts of the b-isox chemical. No precipitation was observed for GFP and dose-dependent precipitation was observed for GFP linked to the SR domain of SRSF2. Panel A shows the result of Western blotting assays. Panel B shows Coomassie stained gel. (C) Western blot assays using antibodies specific to either GFP (lower blot) or to the phosphorylated state of SR repeats. Strong evidence of SR phosphorylation was observed when the GFP fusion to the SR domain of SRSF2 was exposed to the CLK2 enzyme, but no phosphorylation was observed when the fusion protein was exposed to the CDK7 protein kinase enzyme. (D) mCherry:hnRNPA2 hydrogel droplets were exposed to both GFP:SRSF2 and a form of the CLK2 protein kinase carrying an SR domain. Upon exposure to ATP alone, the hydrogel-bound GFP:SRSF2 was released (left panel). When the same experiment was conducted using a form of CLK2 that lacked an SR domain, provision of ATP failed to release the bound GFP:SRSF2 (right panel).

Fig. S2. Amino acids sequences of native and S-to-G mutated SR domains of SRSF2. Figure shows a schematic diagram of the SR domain of SRSF2 (left) and amino acid sequence of either native or S-to-G mutant SRSF2 proteins (right). Serines in the first or second SR domains of SRSF2 were substituted to glycines to generate $SRSF2_{G1}$ or $SRSF2_{G2}$, respectively. These two mutants were recombined to generate $SRSF2_{G1/G2}$ that has S-to-G substitution in both SR domains.

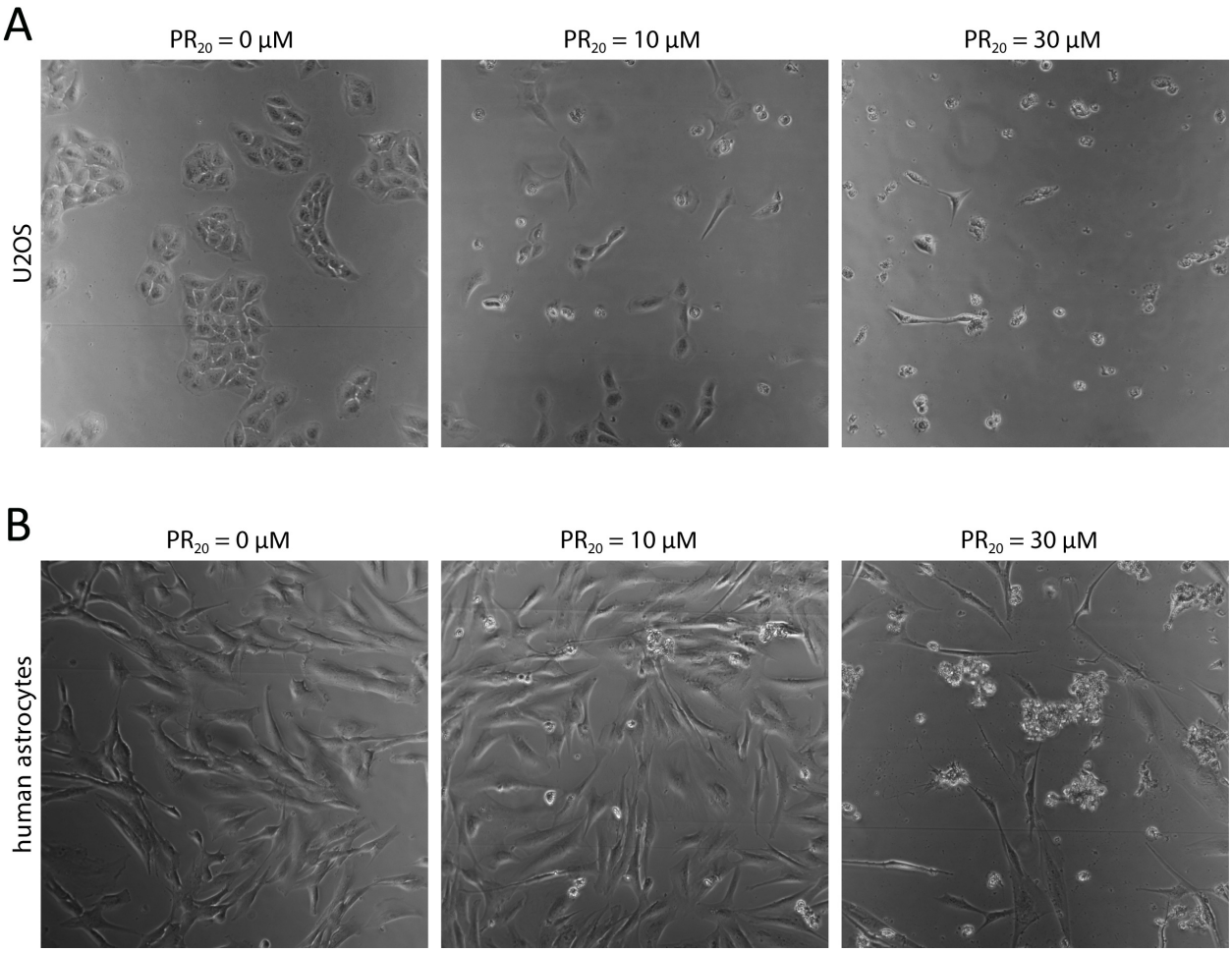

Fig. S3. Phase contrast phase live cell images of U2OS cells and human astrocytes incubated with PR_{20} peptide. U2OS cells (A) or human astrocytes (B) were seeded in chamber slides. After overnight incubation, cells were treated with 0, 10, or 30 µM of PR_{20} peptide. Live cell images were taken using EVOS^{TM} fl microscope (AMG) 24 hours after PR_{20} application.

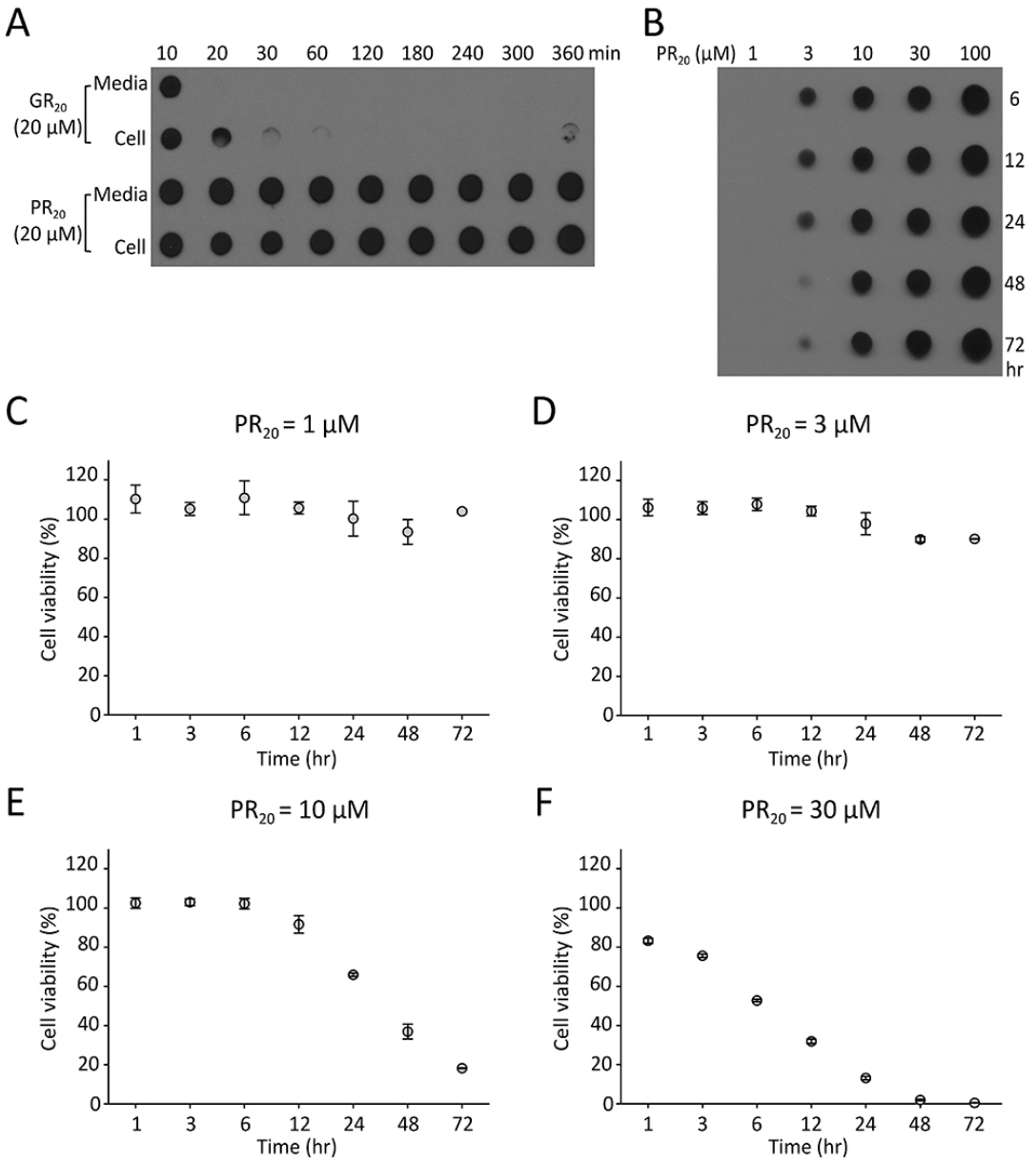

Fig. S4. Measurements of the half-lives of HA tagged GR_{20} and PR_{20} synthetic peptides. (A) Time-dependent decay of GR_{20} and PR_{20} peptides applied to cultured U2OS cells at a concentration of 20 μM. Peptide levels were measured in either culture medium or cells. At each time point, growth medium was transferred to 1.5 ml tube and mixed with SDS loading buffer. Cells were washed with PBS and also lysed with SDS loading buffer. Dot blotting was performed and GR_{20} or PR_{20} peptides were detected using anti-HA antibodies. (B) Time-dependent decay of PR_{20} peptide exposed to cultured U2OS cells grown in 96 well microtiter plates. Cells were treated with indicated concentration of PR_{20} peptide and

incubated for indicated time periods. At each time point, cells were washed and lysed with SDS loading buffer, followed by dot blotting using anti-HA antibodies. (C-F) Time-dependent cell death by different amounts of the PR_{20} synthetic peptide. U2OS cells grown in 96 well plates were incubated with 1, 3, 10, or 30 μM of PR_{20} peptide. At indicated time points, cell viability was analyzed as described in the Materials and Methods.

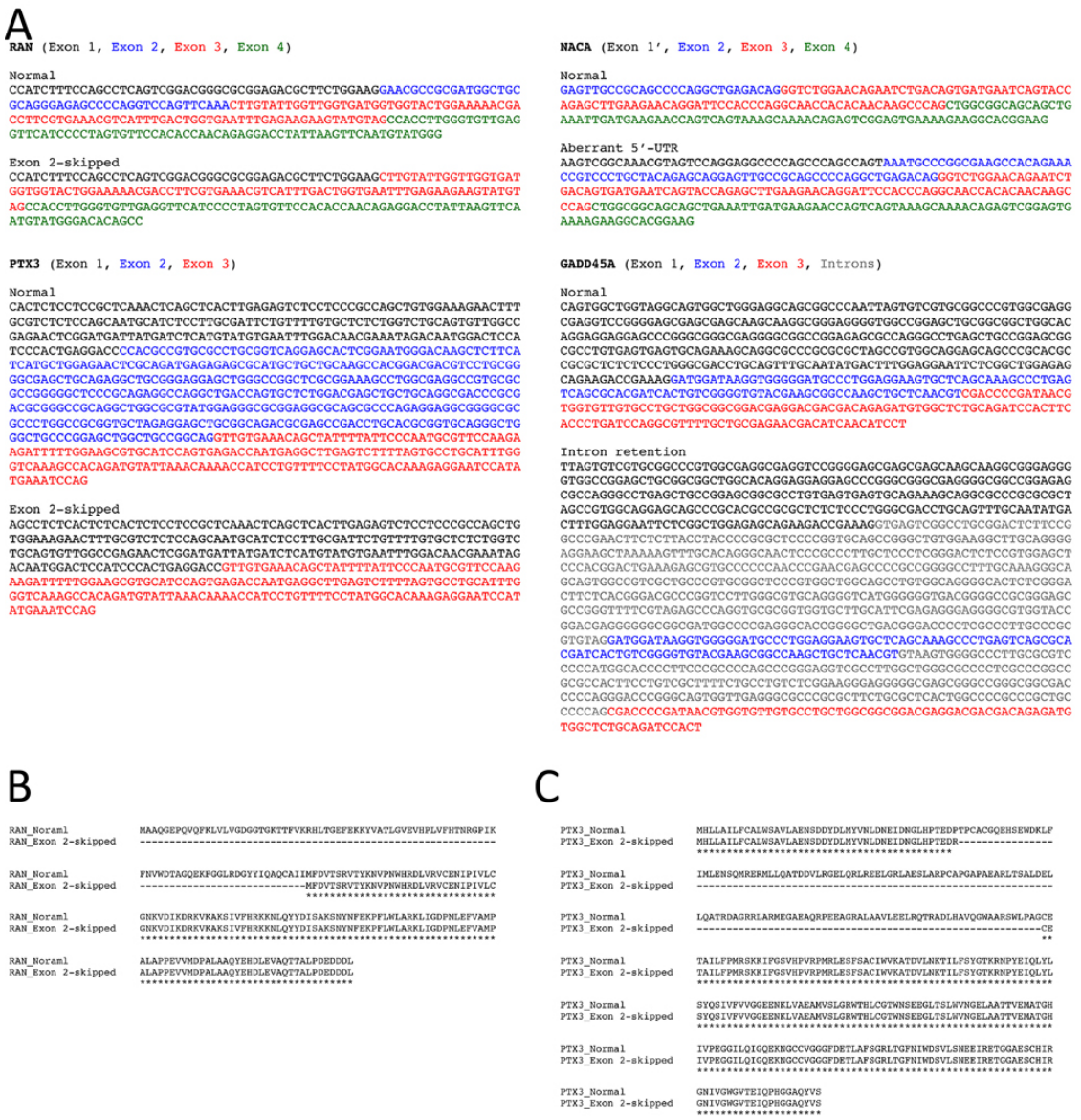

Fig. S5. Nucleotide sequences of normal and aberrantly spliced forms of RAN GTPase, PTX3, NACA and GADD45A mRNAs. (A) DNA sequencing of PCR products of normal and abnormal spliced versions of RAN, PTX3, NACA and GADD45A mRNAs. Different exons of the mRNAs are color-coded to highlight regions aberrantly spliced as a function of cell exposure to the PR_{20} peptide. (B) Predicted changes in the translation of RAN as a function of normal or abnormal splicing. (C) Predicted changes in the translation of PTX3 as a function of normal or abnormal splicing.

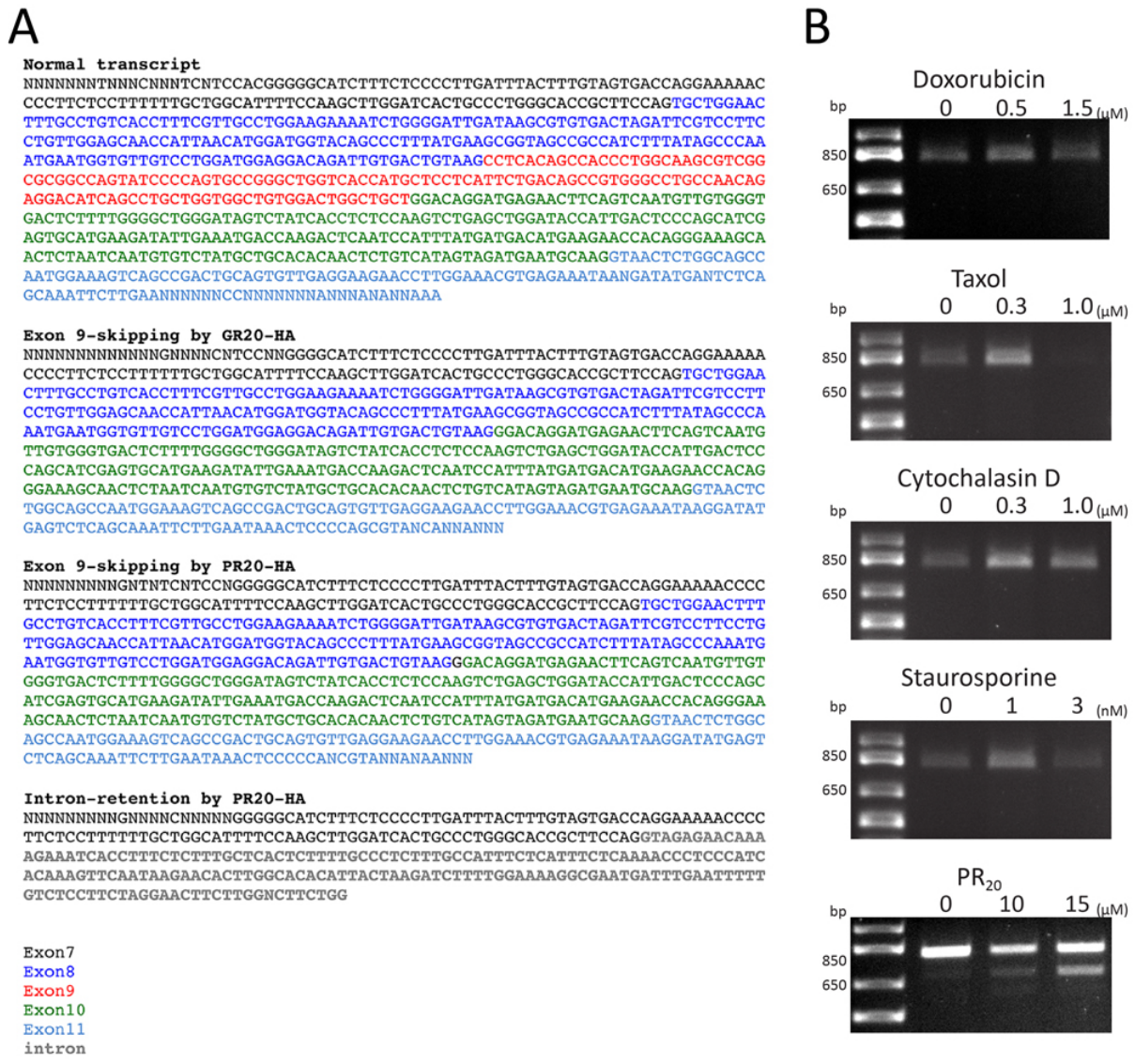

Fig. S6. Sequencing results of aberrantly spliced EAAT2 transcripts. (A) PCR products of the normal EAAT2 transcript, the exon 9-skipping variant, and the intron 7-retention variant as deduced by DNA sequencing. (B) Human astrocytes exposed to four generic toxins, including doxorubicin, taxol, cytochalasin D and staurosporin failed to generate aberrant EAAT2 splicing variants analogous to those generated by the PR_{20} peptide.

Table S1. RNA-seq data of human astrocytes exposed to PR_{20} synthetic peptide.

The table is provided separately as an Excel spread sheet.

References and Notes

1. M. DeJesus-Hernandez, I. R. Mackenzie, B. F. Boeve, A. L. Boxer, M. Baker, N. J. Rutherford, A. M. Nicholson, N. A. Finch, H. Flynn, J. Adamson, N. Kouri, A. Wojtas, P. Sengdy, G. Y. Hsiung, A. Karydas, W. W. Seeley, K. A. Josephs, G. Coppola, D. H. Geschwind, Z. K. Wszolek, H. Feldman, D. S. Knopman, R. C. Petersen, B. L. Miller, D. W. Dickson, K. B. Boylan, N. R. Graff-Radford, R. Rademakers, Expanded GGGGCC hexanucleotide repeat in noncoding region of C9ORF72 causes chromosome 9p-linked FTD and ALS. *Neuron* **72**, 245–256 (2011). Medline doi:10.1016/j.neuron.2011.09.011

2. A. E. Renton, E. Majounie, A. Waite, J. Simón-Sánchez, S. Rollinson, J. R. Gibbs, J. C. Schymick, H. Laaksovirta, J. C. van Swieten, L. Myllykangas, H. Kalimo, A. Paetau, Y. Abramzon, A. M. Remes, A. Kaganovich, S. W. Scholz, J. Duckworth, J. Ding, D. W. Harmer, D. G. Hernandez, J. O. Johnson, K. Mok, M. Ryten, D. Trabzuni, R. J. Guerreiro, R. W. Orrell, J. Neal, A. Murray, J. Pearson, I. E. Jansen, D. Sondervan, H. Seelaar, D. Blake, K. Young, N. Halliwell, J. B. Callister, G. Toulson, A. Richardson, A. Gerhard, J. Snowden, D. Mann, D. Neary, M. A. Nalls, T. Peuralinna, L. Jansson, V. M. Isoviita, A. L. Kaivorinne, M. Hölttä-Vuori, E. Ikonen, R. Sulkava, M. Benatar, J. Wuu, A. Chiò, G. Restagno, G. Borghero, M. Sabatelli, D. Heckerman, E. Rogaeva, L. Zinman, J. D. Rothstein, M. Sendtner, C. Drepper, E. E. Eichler, C. Alkan, Z. Abdullaev, S. D. Pack, A. Dutra, E. Pak, J. Hardy, A. Singleton, N. M. Williams, P. Heutink, S. Pickering-Brown, H. R. Morris, P. J. Tienari, B. J. Traynor; ITALSGEN Consortium, A hexanucleotide repeat expansion in C9ORF72 is the cause of chromosome 9p21-linked ALS-FTD. *Neuron* **72**, 257–268 (2011). Medline doi:10.1016/j.neuron.2011.09.010

3. C. Lagier-Tourenne, M. Baughn, F. Rigo, S. Sun, P. Liu, H. R. Li, J. Jiang, A. T. Watt, S. Chun, M. Katz, J. Qiu, Y. Sun, S. C. Ling, Q. Zhu, M. Polymenidou, K. Drenner, J. W. Artates, M. McAlonis-Downes, S. Markmiller, K. R. Hutt, D. P. Pizzo, J. Cady, M. B. Harms, R. H. Baloh, S. R. Vandenberg, G. W. Yeo, X. D. Fu, C. F. Bennett, D. W. Cleveland, J. Ravits, Targeted degradation of sense and antisense C9orf72 RNA foci as therapy for ALS and frontotemporal degeneration. *Proc. Natl. Acad. Sci. U.S.A.* **110**, E4530–E4539 (2013). Medline doi:10.1073/pnas.1318835110

4. S. Mizielinska, T. Lashley, F. E. Norona, E. L. Clayton, C. E. Ridler, P. Fratta, A. M. Isaacs, C9orf72 frontotemporal lobar degeneration is characterised by frequent neuronal sense and antisense RNA foci. *Acta Neuropathol.* **126**, 845–857 (2013). Medline doi:10.1007/s00401-013-1200-z

5. T. Zu, Y. Liu, M. Bañez-Coronel, T. Reid, O. Pletnikova, J. Lewis, T. M. Miller, M. B. Harms, A. E. Falchook, S. H. Subramony, L. W. Ostrow, J. D. Rothstein, J. C. Troncoso, L. P. Ranum, RAN proteins and RNA foci from antisense transcripts in C9ORF72 ALS and frontotemporal dementia. *Proc. Natl. Acad. Sci. U.S.A.* **110**, E4968–E4977 (2013). Medline doi:10.1073/pnas.1315438110

6. T. Zu, B. Gibbens, N. S. Doty, M. Gomes-Pereira, A. Huguet, M. D. Stone, J. Margolis, M. Peterson, T. W. Markowski, M. A. Ingram, Z. Nan, C. Forster, W. C. Low, B. Schoser, N. V. Somia, H. B. Clark, S. Schmechel, P. B. Bitterman, G. Gourdon, M. S. Swanson, M. Moseley, L. P. Ranum, Non-ATG-initiated translation directed by microsatellite expansions. *Proc. Natl. Acad. Sci. U.S.A.* **108**, 260–265 (2011). Medline doi:10.1073/pnas.1013343108

7. P. E. Ash, K. F. Bieniek, T. F. Gendron, T. Caulfield, W. L. Lin, M. Dejesus-Hernandez, M. M. van Blitterswijk, K. Jansen-West, J. W. Paul 3rd, R. Rademakers, K. B. Boylan, D. W. Dickson, L. Petrucelli, Unconventional translation of C9ORF72 GGGGCC expansion generates insoluble polypeptides specific to c9FTD/ALS. *Neuron* **77**, 639–646 (2013). Medline doi:10.1016/j.neuron.2013.02.004

8. C. J. Donnelly, P.-W. Zhang, J. T. Pham, A. R. Heusler, N. A. Mistry, S. Vidensky, E. L. Daley, E. M. Poth, B. Hoover, D. M. Fines, N. Maragakis, P. J. Tienari, L. Petrucelli, B. J. Traynor, J. Wang, F. Rigo, C. F. Bennett, S. Blackshaw, R. Sattler, J. D. Rothstein, RNA toxicity from the ALS/FTD C9ORF72 expansion is mitigated by antisense intervention. *Neuron* **80**, 415–428 (2013). Medline doi:10.1016/j.neuron.2013.10.015

9. K. Mori, S. M. Weng, T. Arzberger, S. May, K. Rentzsch, E. Kremmer, B. Schmid, H. A. Kretzschmar, M. Cruts, C. Van Broeckhoven, C. Haass, D. Edbauer, The C9orf72 GGGGCC repeat is translated into aggregating dipeptide-repeat proteins in FTLD/ALS. *Science* **339**, 1335–1338 (2013). Medline doi:10.1126/science.1232927

10. M. Kato, T. W. Han, S. Xie, K. Shi, X. Du, L. C. Wu, H. Mirzaei, E. J. Goldsmith, J. Longgood, J. Pei, N. V. Grishin, D. E. Frantz, J. W. Schneider, S. Chen, L. Li, M. R. Sawaya, D. Eisenberg, R. Tycko, S. L. McKnight, Cell-free formation of RNA granules: Low complexity sequence domains form dynamic fibers within hydrogels. *Cell* **149**, 753–767 (2012). Medline doi:10.1016/j.cell.2012.04.017

11. I. Kwon, M. Kato, S. Xiang, L. Wu, P. Theodoropoulos, H. Mirzaei, T. Han, S. Xie, J. L. Corden, S. L. McKnight, Phosphorylation-regulated binding of RNA polymerase II to fibrous polymers of low-complexity domains. *Cell* **155**, 1049–1060 (2013). Medline doi:10.1016/j.cell.2013.10.033

12. M. B. Roth, C. Murphy, J. G. Gall, A monoclonal antibody that recognizes a phosphorylated epitope stains lampbrush chromosome loops and small granules in the amphibian germinal vesicle. *J. Cell Biol.* **111**, 2217–2223 (1990). Medline doi:10.1083/jcb.111.6.2217

13. K. M. Neugebauer, J. A. Stolk, M. B. Roth, A conserved epitope on a subset of SR proteins defines a larger family of Pre-mRNA splicing factors. *J. Cell Biol.* **129**, 899–908 (1995). Medline doi:10.1083/jcb.129.4.899

14. A. M. Zahler, W. S. Lane, J. A. Stolk, M. B. Roth, SR proteins: A conserved family of pre-mRNA splicing factors. *Genes Dev.* **6**, 837–847 (1992). Medline doi:10.1101/gad.6.5.837

15. K. Colwill, T. Pawson, B. Andrews, J. Prasad, J. L. Manley, J. C. Bell, P. I. Duncan, The Clk/Sty protein kinase phosphorylates SR splicing factors and regulates their intranuclear distribution. *EMBO J.* **15**, 265–275 (1996). Medline

16. P. I. Duncan, D. F. Stojdl, R. M. Marius, K. H. Scheit, J. C. Bell, The Clk2 and Clk3 dual-specificity protein kinases regulate the intranuclear distribution of SR proteins and influence pre-mRNA splicing. *Exp. Cell Res.* **241**, 300–308 (1998). Medline doi:10.1006/excr.1998.4083

17. H. J. Menegay, M. P. Myers, F. M. Moeslein, G. E. Landreth, Biochemical characterization and localization of the dual specificity kinase CLK1. *J. Cell Sci.* **113**, 3241–3253 (2000). Medline

18. B. E. Aubol, R. M. Plocinik, J. C. Hagopian, C. T. Ma, M. L. McGlone, R. Bandyopadhyay, X. D. Fu, J. A. Adams, Partitioning RS domain phosphorylation in an SR protein through the CLK and SRPK protein kinases. *J. Mol. Biol.* **425**, 2894–2909 (2013). Medline doi:10.1016/j.jmb.2013.05.013

19. A. I. Lamond, D. L. Spector, Nuclear speckles: A model for nuclear organelles. *Nat. Rev. Mol. Cell Biol.* **4**, 605–612 (2003). Medline doi:10.1038/nrm1172

20. M. Thiry, Behavior of interchromatin granules during the cell cycle. *Eur. J. Cell Biol.* **68**, 14–24 (1995). Medline

21. P. A. Bubulya, K. V. Prasanth, T. J. Deerinck, D. Gerlich, J. Beaudouin, M. H. Ellisman, J. Ellenberg, D. L. Spector, Hypophosphorylated SR splicing factors transiently localize around active nucleolar organizing regions in telophase daughter nuclei. *J. Cell Biol.* **167**, 51–63 (2004). Medline doi:10.1083/jcb.200404120

22. Materials and methods are available as supplementary materials on *Science* Online.

23. C. L. Lin, L. A. Bristol, L. Jin, M. Dykes-Hoberg, T. Crawford, L. Clawson, J. D. Rothstein, Aberrant RNA processing in a neurodegenerative disease: The cause for absent EAAT2, a glutamate transporter, in amyotrophic lateral sclerosis. *Neuron* **20**, 589–602 (1998). Medline doi:10.1016/S0896-6273(00)80997-6

24. D. Kalderon, B. L. Roberts, W. D. Richardson, A. E. Smith, A short amino acid sequence able to specify nuclear location. *Cell* **39**, 499–509 (1984). Medline doi:10.1016/0092-8674(84)90457-4

25. C. Dingwall, J. Robbins, S. M. Dilworth, B. Roberts, W. D. Richardson, The nucleoplasmin nuclear location sequence is larger and more complex than that of SV-40 large T antigen. *J. Cell Biol.* **107**, 841–849 (1988). Medline doi:10.1083/jcb.107.3.841

26. A. D. Frankel, C. O. Pabo, Cellular uptake of the tat protein from human immunodeficiency virus. *Cell* **55**, 1189–1193 (1988). Medline doi:10.1016/0092-8674(88)90263-2

27. A. R. Haeusler, C. J. Donnelly, G. Periz, E. A. Simko, P. G. Shaw, M. S. Kim, N. J. Maragakis, J. C. Troncoso, A. Pandey, R. Sattler, J. D. Rothstein, J. Wang,

C9orf72 nucleotide repeat structures initiate molecular cascades of disease. *Nature* **507**, 195–200 (2014). Medline doi:10.1038/nature13124

28. L. I. Bruijn, T. M. Miller, D. W. Cleveland, Unraveling the mechanisms involved in motor neuron degeneration in ALS. *Annu. Rev. Neurosci.* **27**, 723–749 (2004). Medline doi:10.1146/annurev.neuro.27.070203.144244

29. P. Sheffield, S. Garrard, Z. Derewenda, Overcoming expression and purification problems of RhoGDI using a family of “parallel” expression vectors. *Protein Expr. Purif.* **15**, 34–39 (1999). Medline doi:10.1006/prep.1998.1003

30. H. L. Ball, P. Mascagni, Chemical synthesis and purification of proteins: A methodology. *Int. J. Pept. Protein Res.* **48**, 31–47 (1996). Medline doi:10.1111/j.1399-3011.1996.tb01104.x

31. C. Trapnell, L. Pachter, S. L. Salzberg, TopHat: Discovering splice junctions with RNA-Seq. *Bioinformatics* **25**, 1105–1111 (2009). Medline doi:10.1093/bioinformatics/btp120

32. C. Trapnell, D. G. Hendrickson, M. Sauvageau, L. Goff, J. L. Rinn, L. Pachter, Differential analysis of gene regulation at transcript resolution with RNA-seq. *Nat. Biotechnol.* **31**, 46–53 (2013). Medline doi:10.1038/nbt.2450

33. C. Trapnell, B. A. Williams, G. Pertea, A. Mortazavi, G. Kwan, M. J. van Baren, S. L. Salzberg, B. J. Wold, L. Pachter, Transcript assembly and quantification by RNA-Seq reveals unannotated transcripts and isoform switching during cell differentiation. *Nat. Biotechnol.* **28**, 511–515 (2010). Medline doi:10.1038/nbt.1621

34. M. A. Stephens, EDF statistics for goodness of fit and some comparisons. *J. Am. Stat. Assoc.* **69**, 730–737 (1974). doi:10.1080/01621459.1974.10480196